Journal of Catalysis **182,** 228–233 (1999)
Article ID jcat.1998.2328, available online at http://www.idealibrary.com on IDEAL®

High-Temperature-Aging-Induced Encapsulation of Metal Particles by Support Materials: Comparative Results for Pt, Pd, and Rh on Cerium–Zirconium Mixed Oxides

G. W. Graham, H.-W. Jen, W. Chun, and R. W. McCabe

Ford Motor Company, MD3179/SRL, P.O. Box 2053, Dearborn, Michigan 48121

Received August 24, 1998; revised November 10, 1998; accepted November 11, 1998

High-temperature-aging-induced deep encapsulation of metal particles by the support material in supported-metal catalysts, recently observed in ceria–zirconia-supported Pd catalysts, is also found in comparable Rh catalysts but not Pt catalysts. Aging temperature and Pd loading thresholds to encapsulation are compared for supported Pd catalysts made from ceria–zirconia of varying surface area stability and composition. © 1999 Academic Press

INTRODUCTION

The deep encapsulation of metal by support material in a supported-metal catalyst due to aging-induced collapse of the support is a particularly serious mode of catalyst deactivation because of its permanence. An example of this phenomenon, in which about one-quarter of the 2.25 wt% Pd loaded onto high-surface-area $Ce_{0.5}Zr_{0.5}O_2$ was effectively lost on aging at 1050°C, has recently been documented (1). Because of the relevance of these materials and aging conditions to current automotive exhaust catalysts (2), this study was extended to include the other important metals, Pt and Rh. The new findings, as well as additional results for Pd on ceria–zirconia where Pd loading, ceria–zirconia surface area stability and composition, and aging conditions were varied, are presented here together with a more detailed analysis of the stress imposed by ceria–zirconia on encapsulated metal particles.

EXPERIMENTAL DETAILS

Some of the supported Pd catalysts were obtained from commercial suppliers, in powder form, and others, as well as supported Pt and supported Rh catalysts, were made in-house using commercially available ceria–zirconia powders. The catalysts made in-house were prepared by impregnation of aqueous solution of metal compounds (chloroplatinic acid, palladium nitrate or palladium tetraamine dinitrate, and rhodium nitrate, all from Alpha) to incipient wetness, followed by drying for 12 h at 55°C and calcination at 600°C for an additional 12 h in a standard muffle furnace. The sources, ceria–zirconia compositions, metal loadings, and other relevant data are summarized in Table 1.

Specific surface areas (BET method) and X-ray diffraction (XRD) patterns (using Cu$K\alpha$ radiation) were obtained with Micromeritics ASAP 2400 and Scintag X1 instrumentation, respectively, following various aging and subsequent thermal treatments of the catalyst. Typically, aging was performed by 12 h of heating at 1050 or 1150°C in a flowing gas mixture containing 1 mol% CO/H_2 ($[CO]/[H_2] = 3/1$) alternating every 10 min with 0.5 mol% O_2; the remainder of the mixture consisted of 0.002 mol% SO_2, 10 mol% H_2O, and balance N_2. This "redox" aging ended with the oxidizing portion of the cycle, followed by 30 min of natural cooling, to about 500°C, under N_2, followed by further natural cooling under air. In a few cases, aging was performed by 12 h of heating at 1050, 1150, or 1250°C in air.

RESULTS

As has been previously reported (1), high-temperature aging of ceria–zirconia-supported Pd catalysts may result in deep encapsulation of sintered Pd metal particles as the surface area of the support decreases. These encapsulated particles cannot participate in catalysis since they are inaccessible to gas-phase molecules, a fact clearly demonstrated by their absolute resistance to bulk oxidation, as revealed most simply by thermogravimetric measurements. Direct visual confirmation of encapsulation was also recently obtained by analytical electron microscopy (3). Here, the simple, though indirect, method of XRD, employed in the prior study (1), is again used to probe for encapsulation of Pt and Rh.

The basis for the XRD method is the change in lattice constant of ceria–zirconia between its partially reduced state, which exists at the high temperatures where sintering of both metal and support take place, and its fully oxidized state, which usually exists under ambient conditions. It is possible to somewhat preserve the partially reduced state, however, by cooling from moderate to room temperature under H_2, as illustrated by the XRD patterns in Fig. 1. The

0021-9517/99 $30.00

TABLE 1

Summary of Catalysts

Designation	Composition (wt%)	Loading (metal) (wt%)	Surface area (m^2/g) Fresh	Aged
ESC100[a]	100% CeO_2	0	77[e]	1.4[f]
		9 (Pd)	114[e]	2.0[f]
JM625[b]	70% CeO_2–30% ZrO_2	2.25 (Pd)	—	3.8[g]
DSCI[c]	73% CeO_2–27% ZrO_2	0	88[e]	6.5[g]
				0.9[f]
		2 (Pd)	—	—
		4 (Pd)	130[e]	5.9[g]
				1.8[f]
		8 (Pt)	—	—
		4 (Rh)	—	—
CZ3[d]	70% CeO_2–30% ZrO_2	0	75[e]	7.1[g]
				2.1[f]
		2 (Pd)	79[e]	7.4[g]
		4 (Pd)	—	—
ESC25[a]	25% CeO_2–75% ZrO_2	0	63[e]	5.0[g]
		9 (Pd)	52[e]	5.4[g]

[a] Support and catalyst provided by Engelhard.
[b] Catalyst provided by Johnson Matthey.
[c] Support provided by Degussa; catalysts made in-house.
[d] Support provided by Rhodia (Rhone–Poulenc); catalysts made in-house.
[e] Calcined at 600°C for 12 h.
[f] Redox aged at 1150°C.
[g] Redox aged at 1050°C.

top pattern, labeled "reduced," was obtained from a ceria–zirconia-supported Pd catalyst which had first been aged at 1150°C and then reduced by heating at 500°C for 30 min followed by cooling to room temperature in 0.5 mol% H_2 (balance N_2). The bottom pattern, labeled "oxidized," was obtained from the same aged catalyst but following an additional 2 h of heating at 700°C in air, which ensures that both the unencapsulated Pd and the ceria–zirconia are fully oxidized. The shift in position of the ceria–zirconia diffraction peaks between the two patterns, corresponding to a change in lattice constant of 1%, reflects the presence of some Ce^{3+} cations (which are about 10% larger than Ce^{4+}) in the reduced catalyst. As a consequence of the ceria–zirconia contraction, from its high-temperature partially reduced state, where encapsulation of Pd particles takes place, to its ambient fully oxidized state, the encapsulated Pd particles are subjected to a compressive stress which causes a measurable change in their lattice constant as well. This is illustrated by the XRD patterns in Fig. 2, which are expanded regions from Fig. 1. The peak at 40.1° in the top pattern is from the Pd(111) reflection, and it appears at its expected position in the reduced catalyst. The peak at 40.5° in the bottom pattern is also from the Pd(111) reflection, but it is shifted by an amount that corresponds to a 1% decrease in lattice constant. (The compressive stress applied by the ceria–zirconia in this case is 5.5 GPa, according to an analysis given in the Appendix.) The relative intensities of the

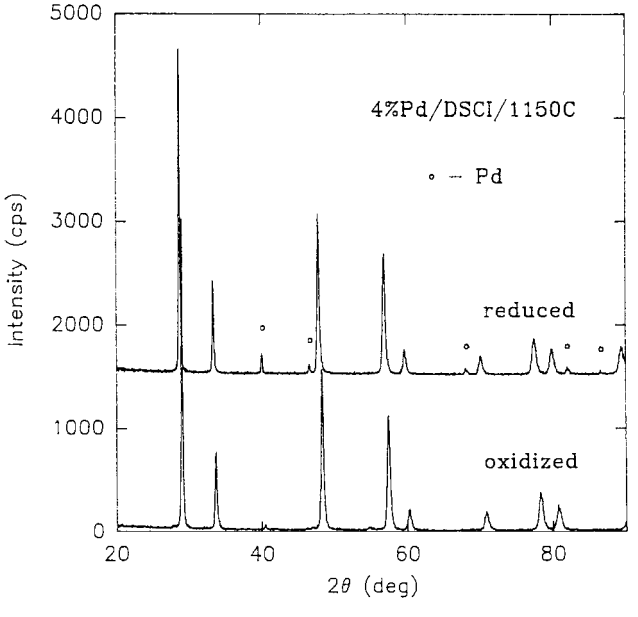

FIG. 1. XRD patterns obtained from a catalyst consisting of 4 wt% Pd on DSCI (73 wt% CeO_2–27 wt% ZrO_2), "redox" aged at 1150°C and subsequently reduced and oxidized. The shift to lower angle of the ceria–zirconia diffraction peaks in the reduced catalyst relative to the oxidized catalyst refects a change in lattice constant.

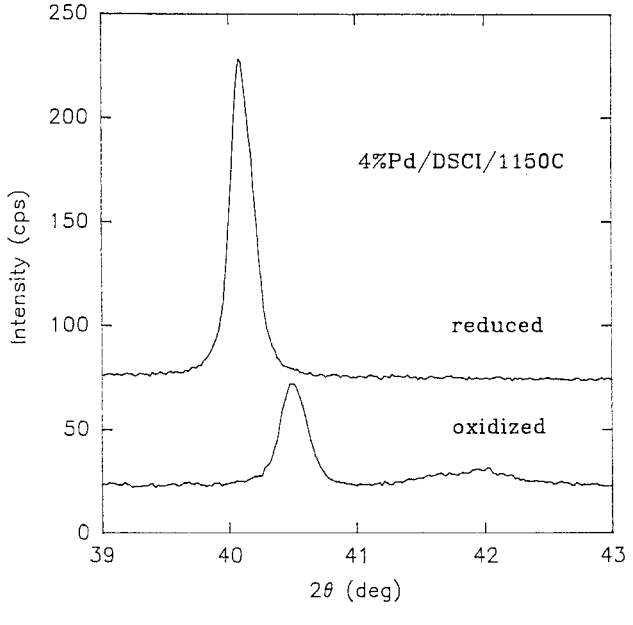

FIG. 2. Enlarged region about the Pd(111) diffraction peak position, taken from the XRD patterns of Fig. 1, illustrating stress-induced shift caused by encapsulation of a fraction of the Pd particles. The broad feature centered near 42° in the bottom pattern is due mostly to the PdO(110) diffraction peak at 41.9° but is also partly due to a weak diffraction peak from ceria–zirconia at 41.6°.

TABLE 2

Summary of Material Properties

Material	Young's modulus (GPa)	Poisson's ratio	Thermal expansion (K^{-1})
CeO_2[a]	≈165	≈0.3	$\approx 11 \times 10^{-6}$
ZrO_2[b]	≈190	≈0.3	—
Pt[c]	168	0.377	8.8×10^{-6}
Pd[c]	121	0.390	11.8×10^{-6}
Rh[c]	375	0.260	8.2×10^{-6}

[a] Ref. (5).
[b] Ref. (6).
[c] Ref. (7).

(111) peaks between the top and bottom patterns provide a measure of the encapsulated fraction of Pd. Most of the broad peak at 41.9° in the bottom pattern is from the PdO (110) reflection.

The mere presence of the Pd metal phase in the oxidized catalyst of Fig. 2, like the thermogravimetric measurements, provides solid evidence for encapsulation. A similar test could also be applied to a Rh catalyst. The shift in peak position, however, is essential to applying the method to a Pt catalyst, since formation of bulk Pt oxides under corresponding conditions would not occur. Given the roughly similar material properties of Pt, Pd, and Rh, listed in Table 2, stress-induced shifts in the position of their (111) diffraction peaks should be comparable, according to the analysis given in the Appendix. As shown in Fig. 3, there is a shift of about 0.5° in the case of Rh but none in the case of Pt, where no difference between the XRD patterns produced by reduced and oxidized catalysts could be detected. For comparison, XRD patterns from the Pd catalyst of Fig. 2 are reproduced in Fig. 3. Since all three catalysts contain nearly the same molar concentration of supported metal, and the Pt pattern has already been scaled down by a factor of 3 to account for its larger X-ray scattering cross section, the similar intensities obtained from the reduced catalysts indicate that all of the metal is being observed in each case. The fraction of Rh encapsulated is apparently about the same as that of Pd, roughly 30%. Judging from the widths of the diffraction peaks, the Pt and Rh particles are of comparable size, although somewhat smaller than the Pd particles.

Turning now to comparisons among Pd catalysts made with differing ceria–zirconia support materials, Fig. 4 contains XRD patterns obtained from three sets of catalysts, all made with ceria–zirconia of nearly the same composition, approximately 70 wt% CeO_2 and 30 wt% ZrO_2, but exhibiting different encapsulation behavior. In all cases the catalysts were heated at 700°C for 2 h in air (i.e., oxidized) after aging. The top two patterns show the effect of aging temperature, 1050 versus 1150°C, on a catalyst of 2.25 wt% Pd loading. The middle two patterns show the effect of Pd loading, 2 and 4 wt%, at a fixed aging temperature of 1150°C. In this case, there was no evidence for encapsulation with a Pd loading of 1 wt%. Furthermore, there was no evidence for encapsulation with any of the Pd loadings when aged at

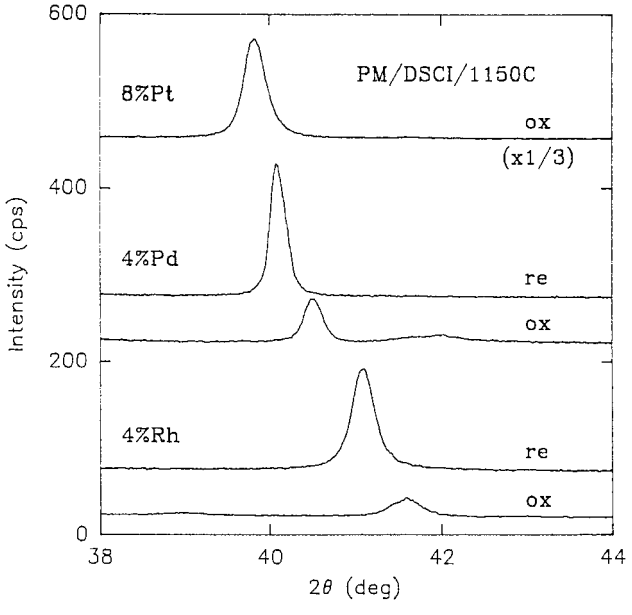

FIG. 3. XRD patterns obtained from comparably loaded, aged, and subsequently treated Pt, Pd, and Rh catalysts showing no evidence of encapsulation of Pt but comparable levels of encapsulation of Pd and Rh. The XRD pattern from the reduced (re) Pt catalyst was identical to that from the oxidized (ox) Pt catalyst.

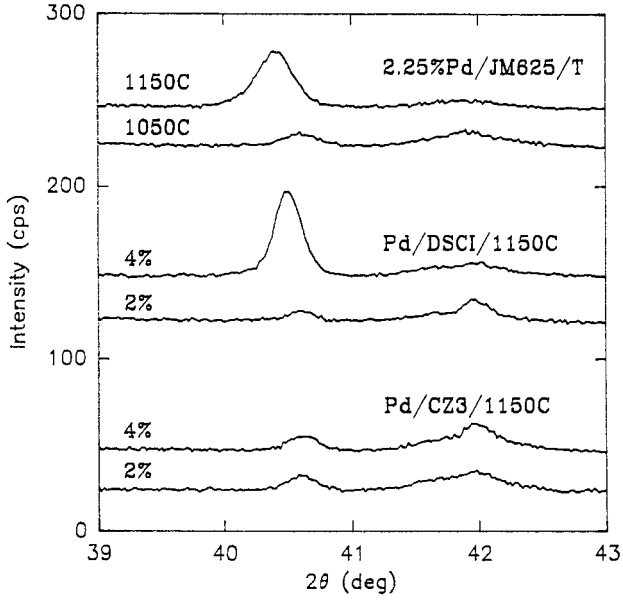

FIG. 4. Pairs of XRD patterns from three sets of Pd catalysts made from different support materials of comparable composition (approximately 70 wt% CeO_2–30 wt% ZrO_2) showing different aging temperature and Pd loading threshold behaviors with respect to Pd encapsulation. In all cases, the catalysts had been oxidized after aging.

1050°C. The bottom two patterns, on the other hand, show no effect of Pd loading when aged at 1150°C. In this case, as well, there was no evidence for encapsulation with either loading when aged at 1050°C. Overall, this series of XRD patterns thus illustrates differences in tendency toward Pd encapsulation, by way of distinct aging temperature and Pd loading threshold behaviors, between comparable support materials. There does appear to be some correlation between the tendency toward Pd encapsulation and the support surface area stability, with the most resistant material retaining the highest surface area, according to Table 1, but the differences in surface area after aging are very slight.

Finally, effects of ceria–zirconia composition and aging environment are illustrated by the XRD patterns shown in Fig. 5. Again, in all cases the catalysts were heated at 700°C for 2 h in air (i.e., oxidized) after aging. The three patterns at the top were all obtained from catalysts consisting of 9 wt% Pd loaded onto pure CeO_2. Roughly 5% of the Pd has been encapsulated after "redox" aging at 1150°C, but there is an indication of some, though less, encapsulation after air aging at 1150°C, as well. Air aging at 1250°C results in two forms of encapsulation, the usual one in which Pd is under stress and a new one in which Pd resists oxidation but apparently is under little or no stress. The pattern at the bottom of Fig. 5 shows that Pd encapsulation also occurs in catalysts made from ZrO_2-rich ceria–zirconia support material. The broad feature centered near 42.5° in this pattern is due to diffraction from the tetragonal structure of this particular ceria–zirconia composition.

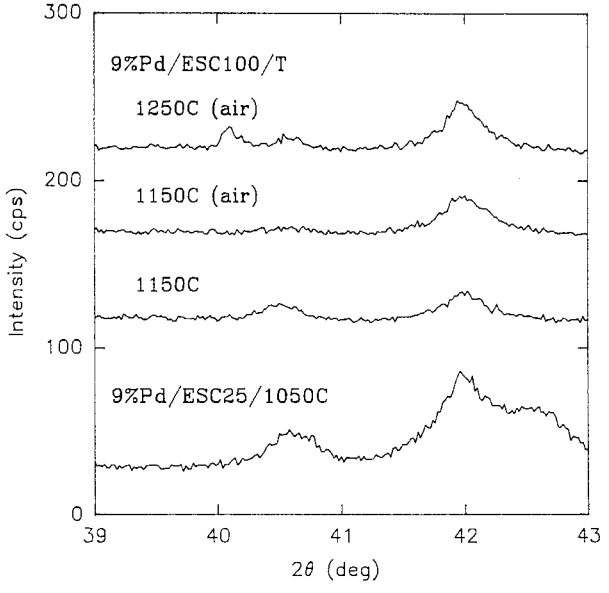

FIG. 5. XRD patterns from Pd catalysts made from pure CeO_2 and ZrO_2-rich ceria–zirconia support materials showing evidence of Pd encapsulation. Again, all the catalysts had been oxidized after aging. The broad feature centered near 42.5° in the bottom pattern is due to a diffraction peak from the ceria–zirconia.

DISCUSSION

It is clear from this study that the deep encapsulation of metal particles by collapsing ceria–zirconia in a supported metal catalyst is a general phenomenon, not limited to Pd, and it thus should be possible to construct a qualitative picture of how it happens on catalyst aging. Viewed sequentially, the overall process begins with the simultaneous sintering of metal and support. The relative rates of these individual processes should certainly be important in determining the end result, and the mode of metal transport could be one of the distinguishing factors involved. For example, the vapor pressure of Pd is quite high, about 10^{-6} Torr, at 1000°C, and thus vapor-phase transport of Pd within the pore structure of the ceria–zirconia could be significant relative to transport via surface diffusion. The vapor pressures of Pt and Rh, on the other hand, are several orders of magnitude lower. Vapor-phase transport of volatile platinum oxides might also occur, but only in an oxidizing aging environment. (This raises the question of whether the outcome for the Pt catalyst would be affected by changing the aging environment to exclusively reducing or even inert, but this was not tested. The possibility that volatile platinum chlorides might participate in the present study was rejected after also examining samples in which chloride remnants from the precursor were eliminated from the fresh catalyst by a low-temperature H_2 treatment before aging.)

It is, perhaps, more remarkable than not that only a fraction of the metal has become encapsulated by the time the support surface area has fallen by a factor of one to two orders of magnitude. At this stage, the metal particles are relatively large and probably even more susceptible to encapsulation because of their limited mobility, but the rate of support surface area loss has also diminished. All three of the metals should be metallic in their condensed state under the most extreme aging conditions used, but differences in surface energy and affinity for oxygen (or metal–support interaction) could produce differences in wetting of the particles by the support material, thus affecting how the particles respond to further collapse of the support. A hypothetical, though reasonable [since the endpoints are consistent with actual XRD and TEM observations (1–3)], Pd particle diameter (solid line) is drawn in Fig. 6 as a function of aging temperature (rather than time) to show how it tends to converge with the average pore diameter (rising dashed line) measured for DSCI. Also shown is the average pore volume (falling dashed line) measured for DSCI, which may be compared with a Pd volume of about 10^{-3} cm^3/g of catalyst for each wt% Pd loading. Ultimately, as the support material approaches its theoretical density through continued sintering, its pore volume will match that of any metal that has not migrated to an external surface. These rough comparisons are suggestive of how small

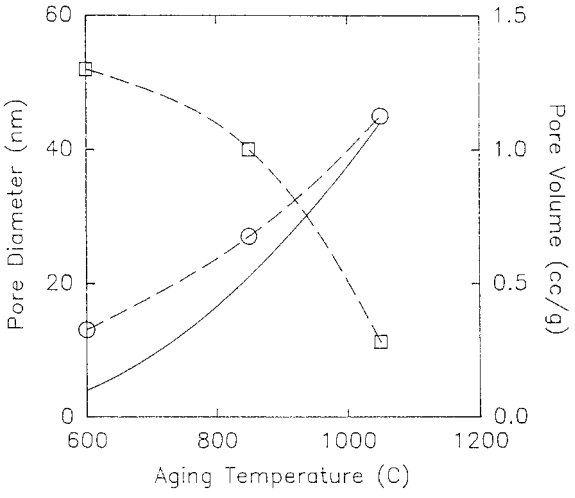

FIG. 6. Average pore diameter (rising dashed line through open circles) and pore volume (falling dashed line through open squares) of DSCI as functions of aging temperature. The solid line is a hypothetical, though reasonable, depiction of average Pd metal particle diameter as a function of aging temperature.

differences in support material properties could have a large effect on the extent of encapsulation near threshold, as illustrated in Fig. 4.

CONCLUSIONS

The deep encapsulation of metal particles by reducible support material in supported metal catalysts due to collapse of the support on high-temperature aging is sensitive to both metal (Pt exhibiting greater resistance than both Pd and Rh in the case of one particular ceria–zirconia material) and support material. Surface area stability, ceria–zirconia composition, and aging conditions can all influence the extent of Pd encapsulation.

APPENDIX

Compressive Stress Applied by Ceria–Zirconia to Encapsulated Metal Particles

The change in lattice constant of ceria–zirconia-encapsulated metal particles arises from a compressive stress applied to the particles by the ceria–zirconia. This stress is due to a differential contraction that occurs primarily because of the change in oxygen content of the ceria–zirconia between high temperature and room temperature. An additional source is the possible difference in thermal expansion coefficients.

In analyzing this situation, it is convenient to use a formula derived for stress and strain in the case of a thick-walled spherical vessel with uniform internal or external pressure (4). [The choice of spherical geometry is consistent with observations of encapsulated particles made by electron microscopy (3).] In its unstrained state, the vessel has an outer radius a and an inner radius b. The vessel material is characterized by its (Young's) modulus of elasticity E and Poisson's ratio ν. Application of a uniform internal pressure q to the vessel causes its inner radius to increase by an amount Δb given by

$$\Delta b = (qb/E)[(1-\nu)(a^3+2b^3)/2(a^3-b^3)+\nu]. \quad [1]$$

In the limit $a \gg b$, this equation becomes

$$\Delta b = (qb/E)[(1+\nu)/2]. \quad [2]$$

It is assumed that this relation describes ceria–zirconia in its fully oxidized state at room temperature.

The metal particle, with unstrained radius c at room temperature and radius $b+\Delta b$ under stress, may be regarded as applying the pressure, q, which can also be expressed in terms of its modulus of elasticity E_m and Poisson's ratio ν_m as

$$\Delta c = (qc/E_\mathrm{m})(1-2\nu_\mathrm{m}). \quad [3]$$

Combining this relation with Eq. [2], to eliminate q, yields

$$\Delta c/c = (\Delta b/b)[2E(1-2\nu_\mathrm{m})/E_\mathrm{m}(1+\nu)]. \quad [4]$$

At high temperature, under the most reducing environment, it is assumed that the metal particle and the ceria–zirconia are in contact, but that they do not apply pressure to each other. Their radii are thus equal. This condition may be expressed in terms of their unstrained room-temperature radii as

$$c(1+k_\mathrm{m}\Delta T) = b(1+k\Delta T+e), \quad [5]$$

where k_m and k are the coefficients of thermal expansion of the metal and the ceria–zirconia, respectively, ΔT is the temperature difference between high temperature and room temperature, and e is the fractional change in linear dimension of the ceria–zirconia due to its change in oxygen content between high temperature (where it is partially reduced) and room temperature (where it is fully oxidized).

Finally, by definition,

$$c - b = \Delta b + \Delta c. \quad [6]$$

Combining this relation with Eqs. [4] and [5], to eliminate b and Δb, yields

$$\begin{aligned}\Delta c/c &= [2E(1-2\nu_\mathrm{m})/E_\mathrm{m}(1+\nu)]\{(k-k_\mathrm{m})\Delta T+e\}/\\ &\{[2E(1-2\nu_\mathrm{m})/E_\mathrm{m}(1+\nu)](1+k\Delta T+e)+(1+k_\mathrm{m}\Delta T)\}\\ &\cong E[e+(k-k_\mathrm{m})\Delta T]/[E+E_\mathrm{m}(1+\nu)/2(1-2\nu_\mathrm{m})], \quad [7]\end{aligned}$$

where the approximation involves dropping all terms higher than first order in the small quantities, e, $k\Delta T$, and $k_\mathrm{m}\Delta T$.

In general, if $E \gg E_m$, then $\Delta b \ll \Delta c$, according to Eq. [4], and almost all of the total differential contraction goes into Δc, according to relation [7]. This case corresponds to the one in which the ceria–zirconia is relatively stiff and unyielding compared with the metal. In the opposite limit, where the metal is by far the stiffer of the two materials, the reverse is true. Typically, however, the total differential contraction is more equally shared between the ceria–zirconia and the metal, their individual strains varying inversely as their respective elastic moduli. Further, the differential-thermal-expansion term may either add to, or subtract from, the term that reflects the change in oxygen content of the ceria–zirconia, depending on the relative size of k and k_m.

Using the numerical values listed in Table 2, relation [7] may be applied to particular cases, such as the Pd catalyst in Fig. 2. Assuming that the elastic properties of DSCI are essentially those of CeO_2 (which are not very different from those of zirconia) and neglecting the difference in coefficient of thermal expansion between CeO_2 and Pd, the value of e deduced from the observed $\Delta c/c$ of 1% is thus 3.2%. Comparable values are obtained from dilatometry measurements of ceria–zirconia (8). Taking this value for e in the case of both the Rh and the Pt catalysts in Fig. 3 leads to predicted values for $\Delta c/c$ of 0.86 and 0.94%, respectively. The observed $\Delta c/c$ of the Rh catalyst is larger, 1.2%, but the significance of this discrepancy is difficult to evaluate in view of the various assumptions and approximations that have been made in this analysis.

Variations in $\Delta c/c$ that accompany variations in metal loading or aging temperature, as shown in Fig. 4, may also reflect other factors not explicitly considered here, such as possible encapsulation at ceria–zirconia grain boundaries (3), where stress could be somewhat relaxed. This is the likely reason for encapsulation of unstressed Pd particles in the case of Pd supported on pure CeO_2 after air aging at 1250°C, as shown in Fig. 5. (The presence of stressed Pd particles as well in this example also demonstrates that a reducing environment is not required for partial reduction of CeO_2 at such high temperatures.) The level of stress supported by the ceria or ceria–zirconia is remarkably high, 5.5 GPa in the case of the Pd catalyst and 9.4 GPa in the case of the Rh catalyst in Fig. 3, according to Eq. [3]. [A previous estimate (1) of this stress was smaller because of an assumed Poisson's ratio for Pd of 0.333.]

Finally, it is necessary to comment on the apparent disparity between the value of e (3.2%) deduced for the Pd catalyst in Fig. 2, which corresponds to the observed change in Pd particle lattice constant, on the one hand, and the fractional change in ceria–zirconia lattice constant (1%) observed on reduction of the catalyst in Fig. 1, which is apparently enough to allow complete relaxation of the stress imposed on the Pd particles, on the other hand. The resolution is thought to involve a possible softening of the ceria–zirconia through the creation of oxygen vacancies, effectively decreasing its modulus so that more of the originally imposed total strain (which is shared between metal and ceria–zirconia) can subsequently be taken up locally (i.e., near the metal particles) by the ceria–zirconia. The detailed picture of this situation could involve clustering of vacancies around the Pd particles.

ACKNOWLEDGMENTS

Sam Tauster (of Engelhard), Paul Andersen (of Johnson Matthey), Dieter Lindner (of Degussa), and Jean-Pierre Cuif (of Rhodia) provided the various catalysts and support materials.

REFERENCES

1. Graham, G. W., Jen, H.-W., Chun, W., and McCabe, R. W., *Catal. Lett.* **44**, 185 (1997).
2. Jen, H.-W., Graham, G. W., Chun, W., McCabe, R. W., Cuif, J.-P., Deutsch, S. E., and Touret, O., *Catal. Today*, in press.
3. Jiang, J. C., Pan, X. Q., Graham, G. W., McCabe, R. W., and Schwank, J., *Catal. Lett.* **53**, 37 (1998).
4. Roark, R. J., and Young, W. C., "Formulas for Stress and Strain," p. 506. McGraw–Hill, New York, 1982.
5. Kilbourn, B. T., "Cerium: A Guide to Its Role in Chemical Technology," p. 12. Molycorp, Inc., 1992.
6. Barsoum, M. W., "Fundamentals of Ceramics," p. 401. McGraw–Hill, New York, 1997.
7. Winter, M., "WebElements" (http://www.shef.ac.uk/chemistry/web-elements/).
8. For example: Sergo, V., Schmid, C., and Meriana, S., *in* "Zirconia '88: Advances in Zirconia Science and Technology" (S. Meriani and C. Palmonari, Eds.), p. 301. Elsevier Applied Science, Amsterdam/New York, 1989.